The influence of Mg doping on the nucleation of self-induced GaN nanowires

F. Limbach, R. Caterino, T. Gotschke, T. Stoica, R. Calarco, L. Geelhaar, and H. Riechert

Citation: AIP Advances 2, 012157 (2012); doi: 10.1063/1.3693394

View online: https://doi.org/10.1063/1.3693394

View Table of Contents: http://aip.scitation.org/toc/adv/2/1

Published by the American Institute of Physics

Articles you may be interested in

Nucleation and growth of GaN nanorods on Si (111) surfaces by plasma-assisted molecular beam epitaxy - The influence of Si- and Mg-doping

Journal of Applied Physics 104, 034309 (2008); 10.1063/1.2953087

From nucleation to growth of catalyst-free GaN nanowires on thin AIN buffer layer

Applied Physics Letters 91, 251902 (2007); 10.1063/1.2817941

Mechanism of molecular beam epitaxy growth of GaN nanowires on Si(111)

Applied Physics Letters 90, 123117 (2007); 10.1063/1.2715119

Optical properties of Si- and Mg-doped gallium nitride nanowires grown by plasma-assisted molecular beam epitaxy

Journal of Applied Physics 104, 074309 (2008); 10.1063/1.2980341

GaN based nanorods for solid state lighting

Journal of Applied Physics 111, 071101 (2012); 10.1063/1.3694674

The influence of AlN buffer over the polarity and the nucleation of self-organized GaN nanowires Journal of Applied Physics **117**, 245303 (2015); 10.1063/1.4923024



The influence of Mg doping on the nucleation of self-induced GaN nanowires

F. Limbach, ¹ R. Caterino, ² T. Gotschke, ¹ T. Stoica, ² R. Calarco, ^{1,a} L. Geelhaar. ¹ and H. Riechert ¹

(Received 18 November 2011; accepted 14 February 2012; published online 29 February 2012)

GaN nanowires were grown without any catalyst by plasma-assisted molecular beam epitaxy. Under supply of Mg, nanowire nucleation is faster, the areal density of wires increases to a higher value, and nanowire coalescence is more pronounced than without Mg. During nanowire nucleation the Ga desorption was monitored insitu by line-of-sight quadrupole mass spectrometry for various substrate temperatures. Nucleation energies of 4.0 ± 0.3 eV and 3.2 ± 0.3 eV without and with Mg supply were deduced, respectively. This effect has to be taken into account for the fabrication of nanowire devices and could be employed to tune the NW areal density. *Copyright 2012 Author(s)*. *This article is distributed under a Creative Commons Attribution 3.0 Unported License*. [http://dx.doi.org/10.1063/1.3693394]

During the last decade, a considerable research effort has focused on semiconductor nanowires (NWs), as they possess the potential for the fabrication of novel nano devices, due to their high aspect ratio at nano scale dimensions and the possibility of integration with silicon-based technology. In particular, III-N NWs are considered suitable for the fabrication of efficient light emitting diodes (LEDs)² but have also been employed for other devices. An approach that allows for high controllability in growing GaN NWs with good structural and optical quality is the catalyst-free growth by molecular beam epitaxy (MBE). In order to grow GaN NWs, higher substrate temperatures and higher V/III ratios are employed compared with normal layer growth. In growth takes place in two phases: the formation of NW nuclei and the subsequent growth of the NWs. Caining control over the initial nucleation phase is critical, as it determines many properties of the GaN NWs such as their density for instance. A delay in the formation of GaN NW nuclei after opening the shutters of the MBE, also called incubation time, has been observed by several groups. Such a delay is also present in the case of catalyst-assisted NW growth. Yet for the GaN NWs grown without any catalyst, the origin of the incubation time during the nucleation process is still under investigation.

In this paper, we report on how the supply of an atomic species, in this case Mg, affects NW nucleation and in particular the duration of the incubation time. Given the paramount importance of the nucleation phase, any additional insight and/or way how to control nucleation is of high relevance both from a fundamental point of view and for applications. More specifically, Mg is commonly used as a p-type doping atom and thus its influence on the growth mechanism of GaN NWs is of importance for the realization of devices within these NWs.³⁰ Even though Mg doping for LEDs is commonly conducted at the end of the growth other devices such as n-Si/p-GaN heterojunctions for heterojunction photovoltaic cells⁵ and p-Si/p-GaN/n-organic hybrid solar cells⁶ might require Mg doping at the beginning of the growth. Moreover, for spin-LEDs it is absolutely necessary to



¹Paul-Drude-Institut für Festkörperelektronik, Hausvogteiplatz 5–7, 10117 Berlin, Germany ²Forschungszentrum Julich, Institute for Bio & Nanosystems IBN and JARA FIT Julich Aachen Research Alliance, 52425 Julich, Germany

^aElectronic mail: calarco@pdi-berlin.de

perform hole injection through the substrate because the spin-lifetime of holes is very short and spin-polarization of the electrons through a ferromagnetic top contact is at the moment inevitable. ^{31,32} Spin-LEDs based on GaN NWs coated by Fe are a potential future application, ³³ and to realize such a device control of Mg doping in the nucleation stage needs to be achieved.

Here, the incubation time and its evolution with the growth temperature are monitored by a line-of-sight quadrupole mass spectrometry (LS-QMS) to detect the Ga desorbing from the substrate and by reflection high-energy electron diffraction (RHEED).²³ These results are correlated with the statistical analysis of the NW areal density of samples grown for short times. We find that NW nucleation occurs much faster under the supply of Mg.

Catalyst-free GaN NWs were grown on Si(111) by plasma-assisted MBE. The N/Ga flux ratio of 6.5 was kept constant for all samples. Prior to growth, the native Si oxide was removed in situ by the deposition of a Ga layer which was subsequently desorbed by raising the temperature until the Si(111) 7×7 reconstruction was observed by means of RHEED, and then the Si surface was nitridated for 5 minutes. Two sets of GaN NW samples were grown. The first set was a time dependence series for the investigation of the nucleation phase with the following growth parameters: substrate temperature (T_S) of 790 °C, nominal growth rate of Ga of 2 nm/min and N of 13 nm/min. For the second set of samples, T_S was varied between 760 °C and 806 °C using the same Ga and N rates employed for the first set. Both series were grown twice, once with Mg supply and once without. The Mg source was set to 300 °C, which yields a beam equivalent pressure of 2.5 · 10^{-8} mbar. The Mg shutter was opened simultaneously with the Ga shutter. Subsequent to growth, scanning electron microscopy (SEM) top view and cross-section images were taken.

Based on the SEM top view images of as-grown samples obtained for different growth durations, a statistical analysis of the areal density of the NWs was carried out. In Fig.1, the NW density on the samples grown under Mg supply (blue squares) and the ones with undoped GaN (green circles) is plotted versus the growth time. Both, the series with Mg supply and the one without show the characteristic behaviour of GaN NW growth described by other authors. $^{20-25}$ In the initial phase, an incubation time can be observed during which no wire growth takes place. Subsequently, the nucleation phase follows, this causes a rapid jump in NW density on the substrate surface to values above $4 \cdot 10^{10}$ cm⁻² in both cases. For longer deposition times, the NW density decreases due to coalescence of closely spaced NWs. 20,35 Widely spaced wires, however, continue to grow separately.

Comparing the results of the two series, it is evident that the nucleation under Mg supply is more rapid. In fact, the maximum NW density is reached earlier than it is the case for the undoped samples. This is underlined by the SEM top view images of the samples grown for 7.5 minutes shown in Fig.1. At the same time the tendency to coalesce is much stronger for the Mg doped wires (GaN:Mg) compared to their undoped counterparts (GaN). This tendency of stronger coalescence has been previously observed and has been linked to an enhanced lateral growth rate. 30, 36, 37 The observation is confirmed by SEM top view images shown in Fig. 1, associated with the samples grown for 20 minutes. The higher absolute NW density during nucleation implies also that the NW nuclei are more closely spaced in the case that Mg is supplied. This phenomenon along with the higher lateral growth rate also drives the observed enhanced coalescence as NWs touch each other much earlier during growth.

Fig.2 shows the typical LS-QMS signal observed for 69 Ga during the nucleation of GaN NWs with and without Mg supply and otherwise identical conditions. The origin of the time axis was chosen to be the opening of the Ga shutter. Prior to this, the signal settles on a background value that is determined by the N_2 supply to the plasma source and its stabilization. Upon opening of the shutters, the 69 Ga signal increases rapidly and settles again at a value which we define as $p_{\rm inc}$, in this case at $1.3 \cdot 10^{-10}$ mbar. The growth stage in which the signal stays constant can be associated with the incubation time, as no RHEED pattern indicating GaN is observed. The absolute level of this signal and the duration of the incubation time depend strongly on the growth temperature as well as the Ga flux. Subsequently, the nucleation phase takes place evidenced by the decrease in the 69 Ga signal. The reason for the decrease of the signal is that the Ga atoms form GaN nuclei and are incorporated into existing nuclei. The rate at which the later process occurs strongly depends on the number of already formed nuclei. Finally, once nucleation has finished, the Ga desorption

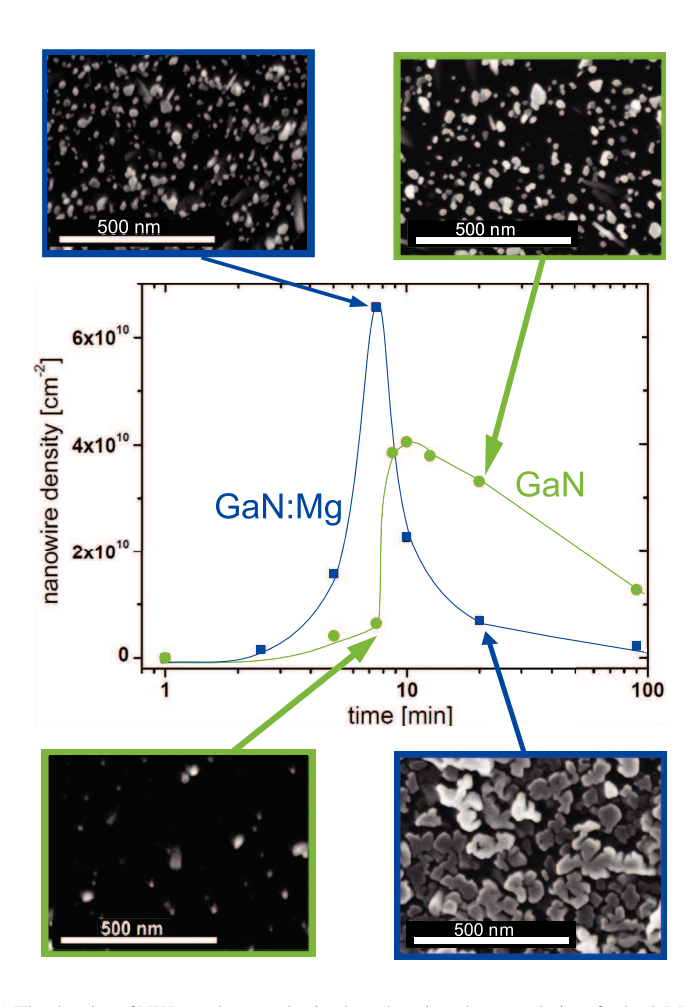


FIG. 1. (color online) The density of NWs on the samples is plotted against the growth time for both Mg-doped (blue squares) and undoped samples (green circles). The insets show SEM top view images of the indicated samples. The lines serve as a guide to the eye only.

and therefore also the incorporation rate stabilize at values which remain constant throughout the entire growth run. For the samples presented in Fig.2, this level we define as p_{stab} is at around $4.5 \cdot 10^{-11}$ mbar. In this stage, the amount of incorporated Ga does not depend on whether Mg is supplied or not.

While the qualitative behaviour of the LS-QMS signal is quite the same for GaN and GaN:Mg a striking difference in the rate with which nucleation occurs is observed. In the case of GaN:Mg, the nucleation phase is much shorter. In order to quantify this nucleation rate, the LS-QMS signal was analyzed in more detail. In particular, the slope of the ⁶⁹Ga desorption decrease is of interest. In the intermediate stage between saturation and incubation time, this decrease is almost linear. As the absolute values of the saturation level may vary due to differences in background pressures, the pressure difference defined as $p_{\text{diff}} = p_{\text{inc}} - p_{\text{stab}}$, is determined. With this information, the times when the LS-QMS signal reaches a partial pressure level of $p(t_1) = (p_{\text{stab}} + \frac{1}{3} \cdot p_{\text{diff}})$ and $p(t_2) = (p_{\text{stab}} + \frac{1}{3} \cdot p_{\text{diff}})$ are extracted. Between these pressure levels, the LS-QMS signal decrease is almost linear in all cases (see Fig.2 for comparison). The difference $\tau = t_2 - t_1$ between these two times gives an indication on the steepness of the signal slope. The bigger τ is the longer it takes to form nuclei and to get into a stable growth regime where supply and incorporation/desorption of Ga do not change anymore over time.

This determination of τ was carried out for all doped and undoped samples grown at different T_S . In Fig. 3, the data are presented in an Arrhenius plot in order to determine the nucleation energy. 38,39

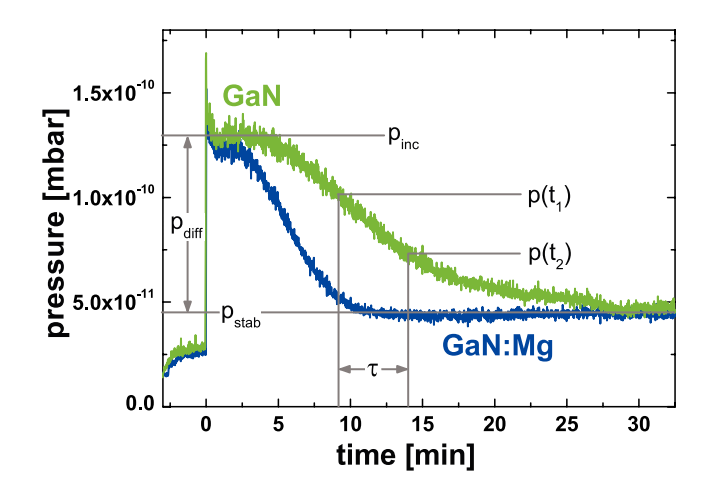


FIG. 2. (color online) The partial pressure of ⁶⁹Ga as detected by the LS-QMS is plotted versus the growth time for two samples, one with (blue) and one without (green) Mg supply.

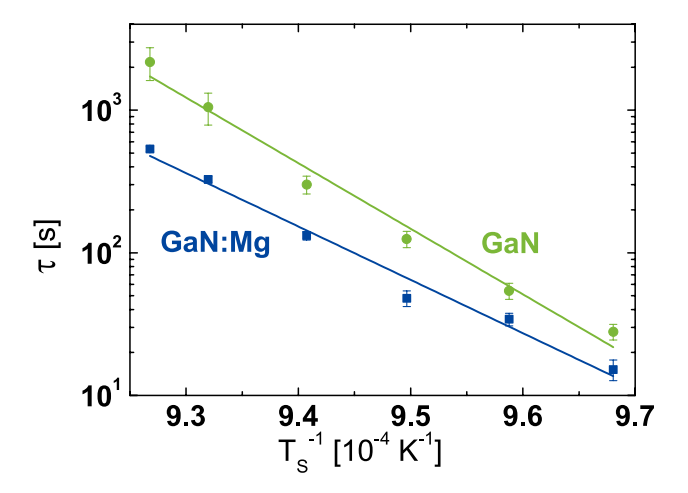


FIG. 3. (color online) Arrhenius plot of τ as defined in Fig. 2 for samples grown with (blue squares) and without (green circles) Mg supply. Both data sets were fitted (solid line) with the exponential function $\tau(T_S^{-1}) = A \cdot \exp(-\Delta E \cdot (k_B T_S)^{-1})$.

Throughout the whole T_S growth window (760 °C - 806 °C), the nucleation rate of the GaN:Mg samples is consistently higher. Moreover, the exponential fit of the respective Arrhenius plot yields a lower nucleation energy for GaN:Mg of 3.2 \pm 0.3 eV compared to the one for GaN of 4.0 \pm 0.3 eV. The absolute value for GaN differs from the one pulished earlier by Consonni *et al.* ²⁵ due to different methods in overcoming the difficulty of temperature calibration.

The interpretation of nucleation energies is not straightforward because they describe the convolution of different phenomena like the activation energy for surface diffusion, activation energy for desorption and the dissociation energy of a critical nucleus.^{38,39} At the same time, those phenomena are not all directly accessible while the nucleation energy is a measurable quantity. Our determination of the nucleation energies with and without Mg shows first of all that there is a systematic difference between the two cases. Moreover, the difference of 0.8 eV between the two energies gives an indication of the stabilizing nature of the Mg atoms: It is evident from the difference in the nucleation energy that GaN:Mg is less sensitive to temperature change than pure GaN. This observation and the enhanced nucleation rate suggest that Mg acts as a stabilizer for the forming nuclei. Lymperakis *et al.* asserted that stoichiometric non-polar GaN surfaces are intrinsically unstable against atomic N and therefore Ga adatom incorporation events are more probable on the c-plane surface.⁴⁰ This balance might shift with Mg acting as a stabilizer for N atoms allowing a higher lateral growth

rate and more rapid nucleation. Such an effect could also explain the enhanced lateral growth rate observed in this study and elsewhere. 36,37

In summary, the nucleation behavior of Mg-doped GaN NWs and their undoped counterparts has been compared. A much more rapid nucleation (shorter incubation time) along with a higher number of NW nuclei is observed if Mg is supplied. Under the employed growth conditions, the energy ΔE for nucleation was deduced to be $\Delta E_{\rm GaN} = 4.0 \pm 0.3$ eV for undoped GaN and $\Delta E_{\rm GaN:Mg} = 3.2 \pm 0.3$ eV for GaN grown with Mg supply.

Beyond the implications for device design and p-type doping of GaN NWs this peculiar nucleation behavior of GaN NWs under Mg supply can be employed to control NW sizes and densities within the self-assembled process. Moreover, the effect might proof to be helpful for controlling selective area growth, where the selectivity is to a large extent determined in the nucleation phase. 14,15,41,42 In particular, selective area growth has been achieved by combining a mask on which the incubation time is very long with holes to an underlying material on which the incubation time is short. As long as the total growth duration is shorter than the incubation time on the mask, NWs grow only in the holes. Thus, the strong effect of Mg on the incubation time that we report here widens the range of possibilities to fine-tune selective area growth. Finally, the effect reported here may very well hold true also for other atomic species. Therefore, the supply of several atomic species during nucleation can be used as a tool to design the NW ensemble according to specific needs.

We are grateful to C. Herrmann, G. Jaschke, and H.-P. Schönherr for their dedicated maintenance of the MBE system and to A.-K. Bluhm for the scanning electron micrographs. This work has been partly funded by the German government BMBF project MONALISA (Contract No. 01BL0810). We thank C. Somaschini for careful reading of the manuscript.

```
<sup>1</sup>C. M. Lieber and Z. L. Wang, MRS Bulletin 32, 99 (2007).
 <sup>2</sup> A. Kikuchi, M. Kawai, M. Tada, and K. Kishino, J. J. of Appl. Phys. P.2 43, L1524 (2004).
 <sup>3</sup> Y. Huang, X. Duan, Y. Cui, and C. Lieber, Nano Lett. 2, 101 (2002).
 <sup>4</sup>J. Ebbecke, S. Maisch, A. Wixforth, R. Calarco, R. Meijers, M. Marso, and H. Lüth, Nanotechnology 19, 275708 (2008).
 <sup>5</sup> Y. B. Tang, Z. H. Chen, H. S. Song, C. S. Lee, H. T. Cong, H. M. Cheng, W. J. Zhang, I. Bello, and S. T. Lee, Nano Lett.
  8, 4191 (2008).
 <sup>6</sup> Y. Chen, H. Shih, C. Wang, C. Hsieh, C. Chen, Y. Chen, and T. Lin, Opt. Express 19, A319 (2011).
 <sup>7</sup>C. Chéze, L. Geelhaar, O. Brandt, W. Weber, H. Riechert, S. Münch, R. Rothemund, S. Reitzenstein, A. Forchel, T. Kehagias,
  P. Komninou, G. Dimitrakopulos, and T. Karakostas, Nano Research 3, 528 (2010).
 <sup>8</sup> L. Geelhaar, C. Cheze, B. Jenichen, O. Brandt, C. Pfüler, S. Münch, R. Rothemund, S. Reitzenstein, A. Forchel, T. Kehagias,
  P. Komninou, G. Dimitrakopulos, T. Karakostas, L. Lari, P. Chalker, M. Gass, and H. Riechert, IEEE J. Sel. Topics in
  Quantum Electron. 17, 878 (2011).
 <sup>9</sup> M. Yoshizawa, A. Kikuchi, M. Mori, N. Fujita, and K. Kishino, J. J. of Appl. Phys. P.2 36, L459 (1997).
<sup>10</sup> M. Sanchez-Garcia, E. Calleja, E. Monroy, F. Sanchez, F. Calle, E. Munoz, and R. Beresford, J. Cryst. Growth 183, 23
11 R. Meijers, T. Richter, R. Calarco, T. Stoica, H. Bochem, M. Marso, and H. Luth, J. Cryst. Growth 289, 381 (2006).
<sup>12</sup> K. Bertness, A. Roshko, N. Sanford, J. Barker, and A. Davydov, J. Cryst. Growth 287, 522 (2006).
<sup>13</sup> R. Songmuang, O. Landre, and B. Daudin, Appl. Phys. Lett. 91 (2007).
<sup>14</sup>T. Schumann, T. Gotschke, F. Limbach, T. Stoica, and R. Calarco, Nanotechnology 22, 095603 (2011).
<sup>15</sup>T. Gotschke, T. Schumann, F. Limbach, T. Stoica, and R. Calarco, Appl. Phys. Lett. 98, 103102 (2011).
<sup>16</sup>O. Brandt, C. Pfüller, C. Chèze, L. Geelhaar, and H. Riechert, Phys. Rev. B 81, 045302 (2010).
<sup>17</sup> S. Fernández-Garrido, J. Grandal, E. Calleja, M. A. Sánchez-Garciá, and D. López-Romero, J. Appl. Phys. 106, 126102
  (2009).
<sup>18</sup> V. Consonni, M. Knelangen, L. Geelhaar, A. Trampert, and H. Riechert, Phys. Rev. B 81 (2010).
<sup>19</sup> V. Consonni, M. Hanke, M. Knelangen, L. Geelhaar, A. Trampert, and H. Riechert, Phys. Rev. B 83 (2011).
<sup>20</sup>R. Calarco, R. J. Meijers, R. K. Debnath, T. Stoica, E. Sutter, and H. Lüth, Nano Lett. 7, 2248 (2007).
<sup>21</sup> V. Consonni, M. Knelangen, A. Trampert, L. Geelhaar, and H. Riechert, Appl. Phys. Lett. 98, 071913 (2011).
<sup>22</sup> S. D. Carnevale, J. Yang, P. J. Phillips, M. J. Mills, and R. C. Myers, Nano Lett. 11, 866 (2011).
<sup>23</sup> C. Cheze, L. Geelhaar, A. Trampert, and H. Riechert, Appl. Phys. Lett. 97, 043101 (2010).
<sup>24</sup>O. Landre, C. Bougerol, H. Renevier, and B. Daudin, Nanotechnology 20, 415602 (2009).
<sup>25</sup> V. Consonni, A. Trampert, L. Geelhaar, and H. Riechert, Appl. Phys. Lett. 99, 033102 (2011).
<sup>26</sup> R. Mata, K. Hestroffer, J. Budagosky, A. Cros, C. Bougerol, H. Renevier, and B. Daudin, J. Cryst. Growth 334, 177 (2011).
<sup>27</sup> T. Clement, S. Ingole, S. Ketharanathan, J. Drucker, and S. T. Picraux, Appl. Phys. Lett. 89 (2006).
<sup>28</sup> A. F. i. Morral, C. Colombo, G. Abstreiter, J. Arbiol, and J. R. Morante, Appl. Phys. Lett. 92 (2008).
```

²⁹ C. Chéze, L. Geelhaar, A. Trampert, O. Brandt, and H. Riechert, Nano Lett. 10, 3426 (2010).

- ³⁰ T. Stoica and R. Calarco, IEEE J. Sel. Top. Q. Ele. **17**, 859 (2011).
- ³¹ H. Zhu, M. Ramsteiner, H. Kostial, M. Wassermeier, H. Schönherr, and K. Ploog, Phys. Rev. Lett. 87, 16601 (2001).
- ³² A. Hanbicki, B. Jonker, G. Itskos, G. Kioseoglou, and A. Petrou, Appl. Phys. Lett. **80**, 1240 (2002). ³³ C. Gao, R. Farshchi, C. Roder, P. Dogan, and O. Brandt, Phys. Rev. B **83**, 245323 (2011).
- ³⁴B. Heying, R. Averbeck, L. F. Chen, E. Haus, H. Riechert, and J. S. Speck, J. Appl. Phys. **88**, 1855 (2000).
- ³⁵ V. Consonni, M. Knelangen, U. Jahn, A. Trampert, L. Geelhaar, and H. Riechert, Appl. Phys. Lett. **95** (2009).
- ³⁶ F. Furtmayr, M. Vielemeyer, M. Stutzmann, J. Arbiol, S. Estradé, F. Peirò, J. R. Morante, and M. Eickhoff, J. Appl. Phys. 104, 034309 (2008).
- ³⁷F. Limbach, E. O. Schaefer-Nolte, R. Caterino, T. Gotschke, T. Stoica, E. Sutter, and R. Calarco, J. Optoel. Adv. Mat. 12, 1433 (2010).
- ³⁸ B. Lewis and J. C. Anderson, *Nucleation and growth of thin films* (Academic Press, 1978).
- ³⁹ L. I. Maissel and R. Glang, *Handbook of thin film thechnology*, edited by L. I. Maissel and R. Glang (McGraw-Hill Book Company, 1970).
- ⁴⁰ L. Lymperakis and J. Neugebauer, Phys. Rev. B **79**, 241308 (2009).
- ⁴¹ H. Sekiguchi, K. Kishino, and A. Kikuchi, Appl. Phys. Exp. 1, 124002 (2008).
- ⁴² K. A. Bertness, A. W. Sanders, D. M. Rourke, T. E. Harvey, A. Roshko, J. B. Schlager, and N. A. Sanford, Adv. Funct. Mater. 20, 2911 (2010).